

Cite this: *Energy Environ. Sci.*, 2011, **4**, 1606

www.rsc.org/ees

## REVIEW

## Tandem polymer photovoltaic cells—current status, challenges and future outlook

Srinivas Sista,<sup>†</sup> Ziruo Hong,<sup>‡</sup> Li-Min Chen<sup>§</sup> and Yang Yang<sup>\*</sup>

Received 9th December 2010, Accepted 22nd February 2011

DOI: 10.1039/c0ee00754d

In this article, we review general approaches, challenges and solutions, as well as latest research progress, in the field of polymer tandem solar cells. Despite many limiting factors ranging from processing issues to characterization issues, it has been shown that high efficiency and in-depth understanding of tandem cell operation can be achieved *via* smart device design and analysis, and interface engineering. We further discuss in detail the operation principles and design rules of polymer tandem cells, revealing a bright future to reach double-digit power conversion efficiency from polymer tandem cells.

### 1. Introduction

Ever-increasing world energy demand, depleting non-renewable energy resources and disruptive climate change due to greenhouse gases has aroused much interest in alternative renewable energy sources. Solar energy is one of the best available alternatives, for it is both abundant and clean. Discovery of photovoltaic effect in silicon (Si) diode in 1954 dawned the era of modern solid state photovoltaic (PV) technology.<sup>1</sup> Since then Si solar cells have evolved as the most mature photovoltaic technology and represent over 90% of the present day photovoltaic

market worldwide.<sup>2</sup> The PV market is mushrooming at a rate of 48% since 2002 and is the world's fastest growing energy technology. In spite of this tremendous growth in PV sector, energy from PV technology accounts for less than 0.1% of the world energy demand. The primary reason for this is high module and installation costs of silicon photovoltaics. The only way to reduce the cost of Si photovoltaics is to scale the production. Thin film PV technology based on other inorganic materials such as cadmium telluride (CdTe) and copper indium gallium selenide (CIGS) are being explored as cheaper alternative<sup>3–5</sup>

In the past decade a new class of photovoltaics based on organic materials has emerged and are a promising alternative to inorganic solar cells because of their low processing cost, ease of processibility, roll-to-roll processibility for large area devices and mechanical flexibility.<sup>6,7</sup> The low efficiency and shorter lifetime of organic PVs is compensated by their low module cost, which provides a strong impetus to investigate organic photovoltaic (OPV) technology.<sup>8</sup>

Researchers around the world are putting in tremendous efforts to push the efficiencies of polymer solar cells to a value that is

*Department of Materials Science and Engineering, University of California-Los Angeles, Los Angeles, California, 90095. E-mail: yangy@ucla.edu*

<sup>†</sup> Current address: General Electric Global Research Center, Niskayuna, New York 12309, USA

<sup>‡</sup> Current address: Advanced Organic Electronics Research Center, Faculty of Engineering, Yamagata University, Yonezawa, Japan.

<sup>§</sup> Current address: Advanced Technology Materials, Inc., Danbury, Connecticut, 06810, USA

### Broader context

More than 80% of the world's energy consumption comes from burning fossil fuels that have had a detrimental effect on climate and the environment. There is an impending need to develop clean and affordable renewable energy resources for better energy security in the future. Energy from the sun is abundantly available and efforts are on to develop affordable solar cells. Polymer solar cells have attracted much attention owing to their ease of processing, mechanical flexibility, roll-to-roll processibility and potentially lower cost. Despite tremendous advancement in the area of polymer solar cells, efficiencies are still low owing to several efficiency loss mechanisms in single junction cells. Polymer tandem solar cells, where two or more single junction cells that absorb in different wavelength range are connected in tandem, are being explored to overcome the limitations of single junction cells. It was not until recently that progress in polymer tandem cells was retarded because of several challenges and issues such as layer-by-layer solution processibility, optimization of component cells and accurate characterization methods. Recent years have seen tremendous progress in polymer tandem cells owing to the development of efficient materials and accurate characterization methods and better understanding of polymer tandem cells through modeling.

competent with their inorganic counterparts. Various strategies have been applied to enhance the efficiencies of OPV cells that include morphology control of the active layer;<sup>9–11</sup> utilizing low band gap polymers to enhance the short circuit current ( $J_{sc}$ )<sup>12–14</sup> and increasing the open circuit voltage ( $V_{oc}$ ).<sup>15,16</sup>

The best power conversion efficiencies (PCE) that have been reported so far based on single photovoltaic cells is around 7–8%<sup>15,17,18</sup> which is much less than efficiencies that have been achieved for inorganic solar cells with similar band gaps ( $E_g$ ). It is possible to achieve power efficiency close to 10% for single-junction polymer photovoltaics through careful design of donor polymers with appropriate band gap and energy levels.<sup>19</sup>

One of the reasons for low efficiencies is narrow absorption range of organic materials. Fig. 1 shows the absorbance of two highly efficient donor polymers based on a large band gap polymer poly (3-hexylthiophene) (P3HT) ( $E_g = 1.95\text{eV}$ ) and

a low band gap polymer poly[(4,40-bis(2-ethylhexyl)dithieno[3,2-*b*:20,30-*d*]silole)-2,6-diyl-*alt*-(2,1,3-benzothiadiazole)-4,7-diyl] (PSBTBT) ( $E_g = 1.5\text{eV}$ ). In either case the absorption range of polymer is narrow and covers only a fraction of the solar spectrum, as a result of which more than 60% of the solar spectrum remains unabsorbed. Another inherent limitation of organic materials is their low carrier mobility as a result of which the thickness of the active layer in a PV cell has to be limited to a value such that the transit time ( $t_{tr}$ ) is less than the carrier lifetime ( $\tau$ ). This restriction on the film thickness leads to insufficient absorption efficiency even at the peak absorption wavelength range.

Besides these loss mechanisms for organic solar cells in general, another major loss mechanism for single junction solar cells is potential loss due to thermalization of hot carriers created when photons of energy greater than band gap are absorbed.



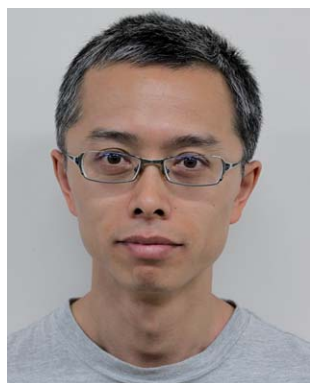
**Srinivas Sista**

*Srinivas Sista is currently working as a research scientist at General Electric Global Research Center, New York. He completed his BS from Institute of Technology—Banaras Hindu University, India in Ceramic Engineering in 2002. He received his PhD in Materials Science & Engineering from Prof. Yang Yang's group at the University of California—Los Angeles in 2010. His doctoral thesis focused on novel organic solar cell device structures for high efficiency.*



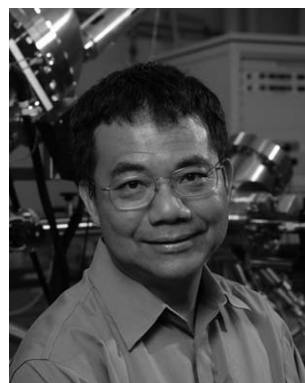
**Li-Min Chen**

*Li-Min (Raymond) Chen obtained his PhD in Prof. Yang Yang's group in the Department of Materials Science and Engineering at the University of California, Los Angeles in 2010. He obtained his BS and MS at National Cheng Kung University (Taiwan) in 2002 and 2004, respectively. His doctoral research is focused on interfaces of polymer solar cells with novel device structures and processing methods as well as transparent conductor applications. He is currently a solar technologist at Advanced Technology Materials Inc. (ATMI).*



**Ziruo Hong**

*Ziruo Hong has been working on organic electronics for more than ten years. He got his PhD (advisor: Prof. Wenian Li) in Condensed Matter Physics from Chinese Academy of Sciences, in 2001. After that, he has been actively working in the field of organic electroluminescence and photovoltaics. He was a post-doctoral researcher leading the organic solar cell team in Prof. Yang Yang's group at UCLA. Currently his research is focused on solution processed organic solar cells. He has authored and co-authored more than 70 research papers.*



**Yang Yang**

*Prof. Yang received his PhD degree in Physics and Applied Physics at the University of Massachusetts, Lowell. After working at the University of California, Riverside as a post-doctoral researcher, and in UNIAX Corporation as a research staff member, he joined University of California, Los Angeles in 1997 as a faculty member. He has been a full professor at UCLA since 2002. His group is working on solution processable electronic devices, including organic and inorganic solar cells, organic LEDs and memory devices, and carbon-based nanomaterials. He has published more than 175 articles in peer-reviewed journals.*

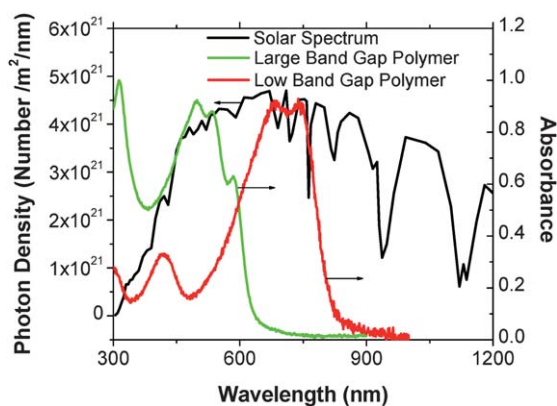


**Fig. 1** Absorbance of P3HT a large band gap polymer (green) and PSBTBT a low band gap polymer (red) is compared to the solar spectrum which spans from 300–1200 nm and even beyond.

The limitations of single junction photovoltaics can be overcome using tandem solar cells where in two or more single cells absorbing in a complementary wavelength range are stacked together. PCE greater than 40% is the highest efficiency obtained to date for triple junction inorganic photovoltaic cells.<sup>20</sup> It has been realized that multi-junction structure is an effective solution to minimize energy loss during photon-to-electron conversion, resulting in theoretical PCE values over 60% from triple junction solar cells.

Several different approaches have been taken by researchers to build organic tandem solar cells either using different processing techniques or device architectures. The most commonly employed device structure is a two terminal monolithic tandem cell in which two sub-cells are connected in series through an interconnecting layer. One of the first reports on two terminal organic tandem cell was by Hiramoto *et al.* where two identical small molecule cells were separated by a thin Au interfacial layer.<sup>21</sup> Small molecule based tandem cells have the advantage that any number of cells can be stacked easily using dry coating process. However, due to the limited choice of small molecule donor materials that have significantly different absorption profiles, hybrid tandem cells using polymer and small molecule sub-cells were explored.<sup>22–26</sup> A more challenging task was to fabricate tandem cell using solution processed component cells because of processibility issues. Several interlayers, both evaporated and solution processed were used to successfully demonstrate tandem cells using polymer sub-cells.

Kawano *et al.* demonstrated one of the first polymer tandem cells using two identical polymer bulk heterojunction (BHJ) sub-cells that were separated by sputter deposited transparent indium tin oxide (ITO).<sup>27</sup> Hadipour *et al.* for the first time fabricated a tandem cell utilizing a low band gap and large band gap polymer BHJ.<sup>28</sup> A major breakthrough in the area of organic tandem cells was the demonstration of all solution processable polymer tandem cells with efficiency over 6% by Kim *et al.*<sup>29</sup> Following this report we demonstrated tandem cells with efficiencies close to 6% using two different polymer BHJs with complementary absorption range.<sup>30</sup> A more detailed report on recent developments in organic tandem cells can be found in ref. 31 and ref. 32. In this review we emphasize the latest progress in this dynamic field.

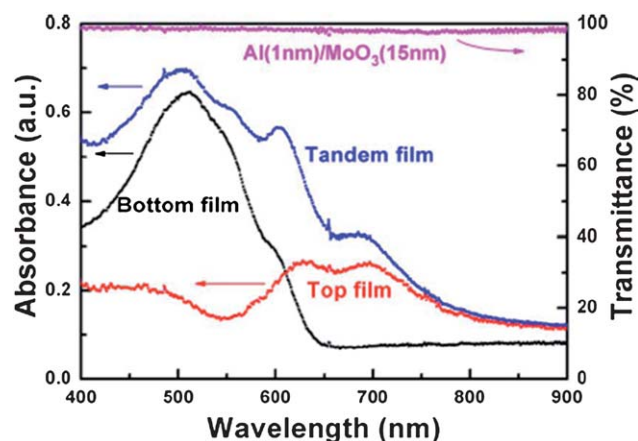


**Fig. 2** Absorbance of top small molecule cell (CuPc/C<sub>60</sub>) is less than the bottom polymer cell (P3HT:PCBM), creating an imbalance in the photocurrent generated by top and bottom sub-cells. The interlayer using transition metal oxide is almost 100% transparent.<sup>25</sup> Reprinted with permission from reference 25. Copyright 2008 American Institute of Physics.

Efforts to fabricate all solution processed tandem cells is gaining momentum and is a path forward to achieve efficiencies close to 15%.<sup>33</sup> The best efficiencies for tandem cells that have been reported so far are slightly over 7% because of several issues and challenges concerning polymer tandem cells.<sup>29,30,34</sup> Several criteria that need to be considered in order to achieve highly efficient polymer tandem devices include sub cells with minimal absorption overlap, an efficient interlayer for connecting the sub-cells and compatible fabrication process for constructing layer-by-layer structure. Besides, optimization of tandem cell requires careful design of optical field and photovoltaic contribution from the sub-cells. Due to the embedded nature of the interlayer and its non-conductive nature in a 2-terminal tandem cell, characterization of sub-cells independently in a tandem configuration is not possible. Therefore, new ways to characterize tandem cells is necessary to develop better understanding of their operation. In this article we will review some of the challenges and issues concerning the fabrication, design and characterization of solution processed tandem cells. We will also review some novel tandem device structures that have been developed recently either to overcome the fabrication issue or design issues of 2-terminal tandem cells.

## 2. Challenges/issues of solution processed tandem cells

### 2.1. Efficient single cells

For series connection,  $V_{OC}$  of the tandem cell is sum of the  $V_{OC}$  of the component cells assuming no potential losses in the interconnection layer. On the other hand  $J_{SC}$  of tandem cell is limited by the component cell delivering smallest  $J_{SC}$  assuming that the fill factor (FF) is the same for the two component cells.<sup>35</sup> In a more realistic scenario where  $J_{SC}$  and FF differ for the two sub-cells,  $J_{SC}$  of tandem cell is controlled by the cell having higher FF. Also photocurrent generated by component cells in a tandem configuration may differ from the photocurrent generated by

single cells fabricated under same condition, due to spectral overlap between the two component cells and change in optical field distribution due to multilayer structure. Therefore, to get maximum benefit out of a tandem structure, photocurrent balance should be achieved through appropriate choice of materials with differing band gaps and optimization of optical field distribution to harvest most of the solar spectrum. In this section we will review the progress in polymer tandem cell efficiencies that resulted from development of new materials and device optimization.

Due to lack of efficient low band gap polymer cells, initial attempts to utilize polymer solar cells in tandem cells were concentrated on hybrid tandem cells or in tandem cells having identical component cells. In case of the hybrid tandem cell, a polymer BHJ based on P3HT: [6,6]-phenyl-C<sub>61</sub>-butyric acid methyl ester (P3HT:PCBM) was used as the bottom cell while a small molecule cell based on metal (Cu or Zn) phthalocyanine (Pc)/fullerene (C<sub>60</sub>) was used as the top cell. The overall efficiency of the tandem cell though was less than the efficiency of the best reported P3HT:PCBM single cell itself.<sup>9</sup> This was partly because of the small  $J_{SC}$  delivered by the small molecule cell and absorption overlap between the polymer and small molecule cells. As shown in Fig. 2 the absorption efficiency of the small molecule cell is much less than that of the polymer cell, as a result of which the amount of current that the small molecule cell can deliver limits the overall current of the tandem cell. Besides, overlap in the absorption spectra of the small molecule cell and the polymer cell in the wavelength range 400–630 nm, further reduces the current delivered by the small molecule cell in tandem configuration.

In the case where identical polymer BHJ were used as component cells,<sup>27</sup> the thickness of each active layer was optimized such that both front and back cells deliver the same amount of photocurrent in tandem configuration. There are several reports on polymer based tandem cells that used P3HT:PCBM as the component cells.<sup>29,30,36</sup> However, for polymer bulk heterojunctions such as P3HT:PCBM which have high absorption and charge collection efficiencies, tandem cell fabrication using identical sub-cells results in marginal efficiency improvement or even decrease.<sup>37</sup> Sakai *et al.* showed that by using different acceptor materials in which one acceptor has strong absorption in the visible range over the other, efficiency of tandem cells can exceed

that of single cells.<sup>38</sup> Sakai *et al.* were able to achieve efficiencies over 5%, further by optimizing the thickness of bottom and top layers so that each sub-cell absorbs equal number of photons.

Certain polymer systems have poor carrier mobility or poor phase separation in the BHJ, owing to which absorption efficiency is less than 50% under optimized conditions.<sup>14,16</sup> Absorption efficiency of such polymer systems can be enhanced by incorporating them into tandem structures. Dennler *et al.* showed that full potential of tandem cells with similar external quantum efficiency (EQE) can be realized when the two sub-cells have similar band gaps.<sup>33</sup>

A major advantage of tandem solar cells is that the energy loss due to thermalization of carriers can be minimized when a large band gap cell is stacked with a low band gap cell. Hadipour *et al.* demonstrated the first polymer tandem cell using two different polymer BHJ systems with complementary absorption range whose structure is shown in Fig. 3(a).<sup>28</sup> In this work both the bottom anode and the middle electrode were a semitransparent Au layer creating an optical cavity in the bottom cell. The optical cavity was tuned such that there is maximum overlap between the transmission through the bottom cell and the absorption of top low band gap cell as shown in Fig. 3(b). The reported efficiencies were low because the partially reflective metal layers reduce the amount of light absorbed by the sub-cells.

A major breakthrough in the area of polymer tandem cells was when Kim *et al.* demonstrated the first all solution processable polymer tandem cells using two high efficiency single cells.<sup>29</sup> Poly[2,6-(4,4-bis-(2-ethylhexyl)-4*H*-cyclopenta[2,1-*b*:3,4-*b'*]dithiophene)-*alt*-4,7-(2,1,3-benzothiadiazole)] (PCPDTBT) was used as a low band gap polymer and P3HT was used as the large band gap polymer. In addition to donor polymer with complementary absorption range, they used two different acceptor materials PC<sub>60</sub>BM and PC<sub>70</sub>BM. Dennler *et al.* performed optical simulations on tandem cells using the same materials that were used by Kim *et al.*<sup>39</sup> They showed that the decrease in number of photons absorbed by the top cell with increasing thickness of the bottom cell is more pronounced than *vice versa*. Secondly, the combination of the donor and acceptor materials that is used in both top and bottom cells of the tandem cell is very crucial in maximizing the number of photons absorbed by each sub-cell. Dennler *et al.* calculated the number of photons absorbed by the top and bottom cell for various

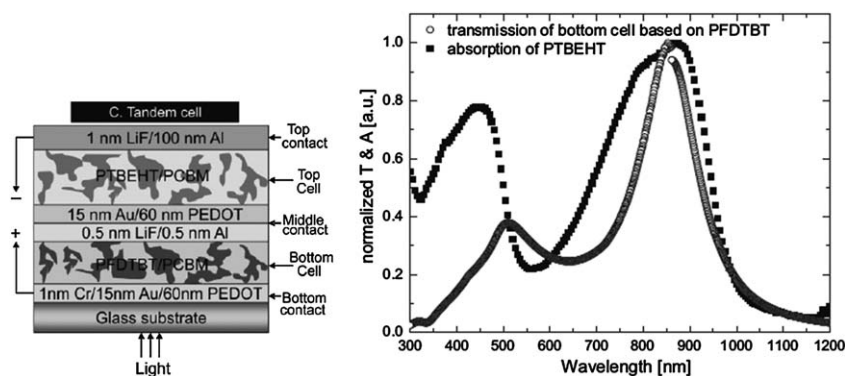


**Fig. 3** (a) First polymer tandem cell using combination of low band gap polymer (PTBEHT) and a large band gap polymer (PFDTBT) system fabricated by Hadipour *et al.* (b) The optical cavity in the bottom PFDTBT cell was optimized such that transmission of PFDTBT coincides with the absorption of top low band gap PTBEHT cell.<sup>28</sup> Reprinted with permission from reference 28. Copyright 2006 Wiley VCH.

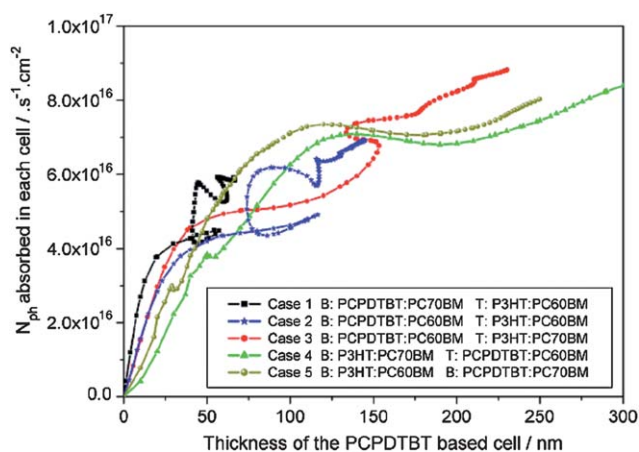


**Fig. 4** Number of photons absorbed by both bottom (B) and top (T) cells as the thickness of low band gap PCPDTBT cell is varied for different combinations of donor and acceptor blends. The combination of PCPDTBT:PC<sub>60</sub>BM as bottom cell and P3HT:PC<sub>70</sub>BM as top cell (red curve) absorbs the most number of photons.<sup>39</sup> Reprinted with permission from reference 39. Copyright 2007 American Institute of Physics.

combinations of donor and acceptor blends as shown in Fig. 4. The maximum number of photons are harvested for the combination of P3HT:PC<sub>70</sub>BM as top cell and PCPDTBT:PC<sub>60</sub>BM as the bottom cell for thickness PCPDTBT cell thicknesses in the range 130–250 nm. This is because the absorption of the bottom PCPDTBT:PC<sub>60</sub>BM cell is minimum in 450–650 nm range where the top P3HT:PC<sub>70</sub>BM cell absorbs as shown in Fig. 5. This observation is in agreement with the experimental results published by Kim *et al.* Although using low band gap polymers as front cell and large band gap as rear cell may help in extracting more solar photons, in theory this is not a desired configuration for tandem cells. An ideal tandem structure would employ a large band gap cell as the front cell instead, to reduce the efficiency loss due to thermalization of hot carriers.

In order to realize tandem polymer solar cells with appropriate layer sequence, and a better understanding of the charge recombination mechanism in the interlayer, Sista *et al.*<sup>30</sup> used a silole substituted low band gap polymer, poly[(4,4'-bis(2-

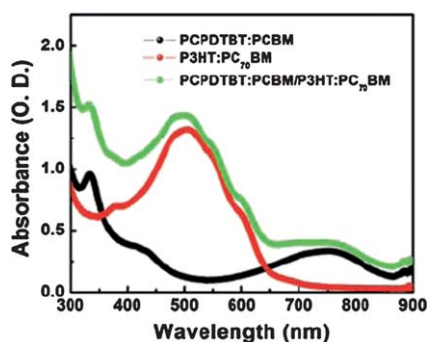


**Fig. 5** Absorption profile of PCPDTBT:PC<sub>60</sub>BM and P3HT:PC<sub>70</sub>BM cells used as sub-cells by Kim *et al.* In the valley in the absorption of PCPDTBT:PC<sub>60</sub>BM cell, P3HT:PC<sub>70</sub>BM cell has maximum absorption. This helps in balanced photocurrent generation in both top and bottom cells.<sup>29</sup> Reprinted with permission from reference 29. Copyright 2007 AAAS.

ethylhexyl) dithieno[3,2-*b*:2',3'-*d*]silole)-2,6-diyl-*alt*-(2,1,3-benzothiadiazole)-4,7-diyl] (PSBTBT) in conjunction with P3HT in the tandem devices. PSBTBT:PC<sub>70</sub>BM single cells show a high FF because the PSBTBT polymer chains pack efficiently leading to strong  $\pi$ - $\pi$  interactions.<sup>40</sup> It was observed that the PCE of PSBTBT:PC<sub>70</sub>BM single cell increases by 10% when the incident light is reduced from 1 sun to  $\frac{1}{2}$  sun because of considerable decrease in non-geminate recombination loss at low light intensities. Taking advantage of this property, Sista *et al.* used PSBTBT:PCBM cell as the rear cell since the light intensity received by the rear sub-cell is attenuated by  $\sim 40\%$  after passing through the front P3HT:PCBM sub-cell. The thickness of the rear sub-cell using PSBTBT:PC<sub>70</sub>BM was unchanged, while photocurrent balance between the two sub-cells was achieved by varying the thickness of the bottom P3HT:PC<sub>70</sub>BM cell. From optical simulations they calculated that the top PSBTBT cell absorbs 15% more photons than the front P3HT cell. The minimal absorption overlap between the PSBTBT and P3HT cells, their high FF and optimized optical field distribution, as well as good interlayer to connect the two sub-cells, led to high efficiency tandem cells with efficiency close to 6%.

Recently, there have been reports on polymer tandem cells using high efficiency low band gap polymers.<sup>41,42</sup> In all the high efficiency tandem cells that have been demonstrated so far, P3HT has been as used as the large band gap polymer. Despite the high mobility and good phase separation in P3HT:PCBM blend, the  $V_{OC}$  generated by such a large band-gap cell is very low. From the empirical relationship developed by Sharber *et al.*,<sup>19</sup> potential limit to  $V_{OC}$  that can be generated by a donor with band gap of 1.9 eV is close to 1.3 V, compared to 0.6 V that is observed for P3HT:PCBM system. Thus by making use of large band gap polymer that delivers  $V_{OC}$  close to the theoretical limit, tandem cell efficiencies can be dramatically improved. Secondly, low band gap polymers that have been developed so far either have low carrier mobility or have unfavorable phase separation when blended with PCBM, leading to low FFs. Therefore, a relatively thin layer of low band gap cells is used to achieve optimal charge collection efficiency, imposing a constraint on the photocurrent tunability of the tandem cell. With better understanding of correlation between molecular design and morphology control, more efficient building blocks should be available for tandem solar cells.

To conclude this section, the criteria for choosing materials for single cells are that: (a) they should have complementary absorption spectrum with minimal absorption overlap; (b) minimal recombination losses in sub-cells; and (c) appropriate energy levels of the donor polymer so that each sub-cell delivers maximum  $V_{OC}$ .

## 2.2. Efficient interconnection layer

In the previous section we have outlined the selection criterion for single cells assuming that the inter-connection layer is functioning efficiently. However, in reality the interlayer connecting the two sub-cells is very critical in the fabrication of highly efficient tandem cells. An inefficient interlayer leads to electrical and/or optical losses and the  $V_{OC}$  of the tandem cell is not equal to the sum of the  $V_{OC}$  of the component cells. The role of the interlayer is twofold: (a) it should efficiently collect electrons

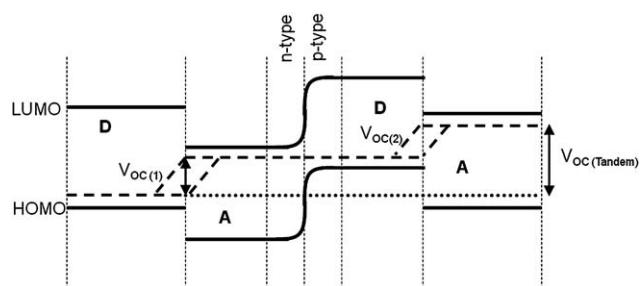


**Fig. 6** Energy level diagram at open circuit for a double heterojunction solar cell using highly doped organic layers as interlayer. Doped organic layers form Ohmic contact with front and back cells and also form an efficient recombination center.<sup>46</sup>

from one sub-cell and holes from another sub-cell; and (b) it should act as an efficient recombination zone free of potential loss for the collected electrons and holes.

**2.2.1 Ohmic contacts with sub-cells.** In case of small molecule tandem cells, the acceptor layer of bottom cell and the donor layer of the top cell should be completely separated to prevent formation of an inverse p-n junction. In early work reported by Yakimov *et al.*,<sup>43</sup> a thin layer of Ag was used as an interlayer that acts as a recombination site for electrons and holes, & also aligns the Fermi levels of the adjacent donor and acceptor layers, adding up the  $V_{OC}$ . It also quenched the inverted junction effectively, such that the two heterojunctions are series connected. However, if a metal nanocluster is used as an interlayer in a tandem cell with at least one polymer BHJ as sub-cell, the interlayer contacts both the acceptor and donor domains of the BHJ. Therefore, selective extraction of an electron or hole from the polymer BHJ is not possible.

An alternative approach that Dennler *et al.* took was to fabricate a diffused bilayer polymer heterojunction instead of a BHJ, so that only PCBM contacts the metal nanoclusters.<sup>22,44</sup> Another approach is to have additional hole blocking and electron blocking layers in the interlayer. In addition to blocking holes (or electrons) the interlayer should be able to collect electrons (or holes) efficiently from the two sub-cells. Drechsel *et al.* proposed that a general approach to establish Ohmic contact between the sub-cells is to use a heavily doped p-n junction as shown in Fig. 6.<sup>45</sup> They proved that highly doped organic layers as recombination contacts in tandem cells are superior to metal cluster based approach.<sup>43</sup> This allowed addition of the  $V_{OC}$  of individual subcells in tandem architectures with minimal loss due to absorption or reflection in the interlayer. More importantly, the connection layers do not depend on the choice of photoactive materials.

Colsmann *et al.* used n-doped and p-doped organic layers on either side of a thin Au layer as hole blocking and electron blocking layer, respectively, as shown in Fig. 7.<sup>23</sup> Lithium doped 4,7-diphenyl-1,10-phenanthroline (BPhen:Li) layer was used as the n-doped layer and 2,5-cyclohexadine-1,4-diylidenedimalononitrile doped 4,4,4-tris(*N*-3-methylphenyl-*N*-phenylaminotriphenylamine (MTDATA:F4TCNQ) was used as the p-doped layer. These doped organic layers also form Ohmic contact for electrons and holes with the bottom polymer cell and

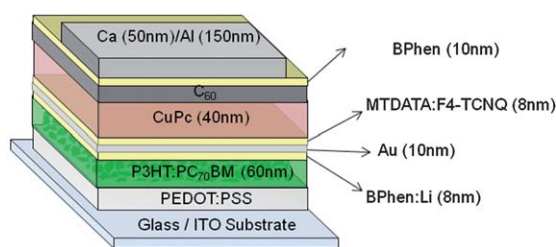


**Fig. 7** Tandem structure using doped organic layers as the interlayer, forming an Ohmic contact with the top and bottom cells. A thin Au layer is inserted between the n-doped and p-doped layer that acts as efficient recombination center.<sup>23</sup>

top small molecule cell, respectively. The thin Au layer acts as a recombination zone for collecting electrons and holes.

More commonly used interlayers for tandem cells are bilayer of low work function (n-type) and high work function (p-type) layers.<sup>24,47</sup> Typical materials used for p-type layer were high work function metal oxides such as molybdenum oxide ( $\text{MoO}_3$ ) or tungsten oxide ( $\text{WO}_3$ ). These metal oxides form good Ohmic contact with organic solar cells and are also highly transparent, making them suitable candidates for interlayer in tandem cell.<sup>48</sup> Zhao *et al.* used  $\text{MoO}_3$  as high work function contact for the top cell and a bilayer of lithium fluoride and aluminium forming a low work function contact with the bottom cell.<sup>47</sup> No optical loss in the interlayer was observed because of almost 100% transmittance of the interlayer as shown in Fig. 2, and no potential losses were observed either.

Fabrication of a small molecule tandem cell or hybrid tandem cell is simpler because the interlayer and the top sub-cell are thermally evaporated. However, a major challenge in fabricating polymer tandem cells is the coating of the top polymer BHJ without damaging the underlying layers. Thus, the major criterion in screening an interlayer besides forming a good Ohmic contact is the robustness of the interlayer so that it can withstand any solution process and protect the bottom polymer BHJ. Kawano *et al.* demonstrated a polymer tandem cell using ITO modified poly-(3,4-ethylenedioxythiophene):poly(styrenesulfonate) (PEDOT) as interlayer.<sup>27</sup> A 20 nm thick sputter deposited ITO was dense enough to protect the bottom polymer cell. However, there was loss in  $V_{OC}$  of the tandem cell compared to the reference single cells, because of high contact resistance at the ITO and bottom cell interface. Hadipour *et al.* used an efficient interlayer consisting of n-type and p-type layers. The n-type layer consisted of a bilayer of  $\text{LiF}(5 \text{ \AA})/\text{Al}(5 \text{ \AA})$  and the p-type contact consisted of bilayer of  $\text{Au}(15\text{nm})/\text{PEDOT}(60\text{nm})$ .<sup>28</sup> Au layer was deposited to protect the bottom  $\text{LiF}/\text{Al}$  contact from the solution process of the top polymer BHJ.  $V_{OC}$  of the tandem cell was equal to the sum of  $V_{OC}$  of the component cells which shows the effectiveness of the interlayer. The disadvantage of using metal interlayers though is loss in transmittance of photons for the back cell.

Efforts thus far were concentrated on interlayers that were thermally evaporated. However, real advantage of polymer solar cells is the ease of fabrication using solution process and all solution processed polymer tandem cells are an attractive alternative. There have been many reports on solution-processed electron transport layers such as  $\text{ZnO}$  and  $\text{TiO}_2$ , that can be used as n-type layers in the interlayer.<sup>49–52</sup> These electron transport

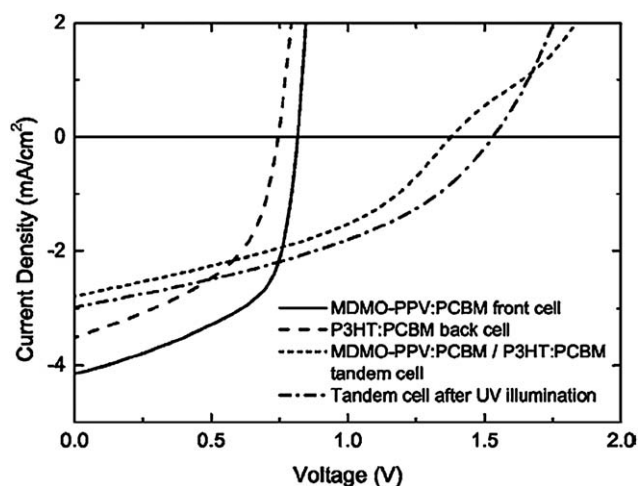


**Fig. 8**  $J$ - $V$  characteristics of single reference cells using P3HT and MDMO:PPV as the donor polymer and tandem cell fabricated using the same polymer system. An s-shape is observed in the  $J$ - $V$  curves of the tandem cell and the s-shape disappears upon UV irradiation.<sup>36</sup> Reprinted with permission from reference 36. Copyright 2007 American Institute of Physics.

layers are wide band gap semiconductors and are highly transparent in the wavelength range where the polymer BHJs absorb. PEDOT, being a high-work-function conducting polymer, is predominantly used to form an Ohmic contact for a hole with the polymer BHJ and is an alternative to thermally evaporated high-work-function metal oxides. The first demonstration of all solution processed polymer tandem cells was by Gilot *et al.*<sup>36</sup> They used zinc oxide (ZnO) nanoparticles (NPs) dissolved in acetone to deposit the n-type layer, while aqueous-based neutral pH PEDOT was used as the p-type layer. ZnO has been shown to form an efficient contact for electron extraction from polymer BHJ<sup>52,53</sup> because of its matching energy level with PCBM. The alcohol based solution of ZnO NPs does not damage the bottom polymer layer and aqueous based PEDOT:PSS layer does not affect the ZnO layer. The thickness of ZnO layer was 30 nm and that of PEDOT was 15 nm. Such an interlayer protects the bottom polymer cell from any subsequent solution process. The entire fabrication process was such that none of the solution process steps damaged the layers underneath. Using these solution processed interlayers, double and triple junction tandem cells were shown with minor losses in  $V_{OC}$ .

Sol-gel derived titanium oxide ( $TiO_2$ ) is another potential candidate as an n-type contact. Kim *et al.* and Sista *et al.* used sol-gel based  $TiO_2$  layer for efficient electron extraction from the bottom cell and PEDOT as a p-type layer.<sup>29,30</sup> Though the synthesis approaches of  $TiO_2$  employed by the two groups are totally different, highly efficient tandem cells were demonstrated without voltage losses. Kim *et al.* used a  $TiO_x$  precursor solution to coat 20–30 nm thick dense films on polymer layer that was followed by baking in air for hydrolysis of precursor into solid state  $TiO_x$ . The purpose of the  $TiO_x$  layer was manifold: being an electron transport layer, a hole blocker and an optical spacer. On the other hand Sista *et al.* used crystalline nanoparticles of  $TiO_2$  dispersed in alcohol solvent, to form an electron transport layer.<sup>50</sup> Several other reports on solution processed tandem cells

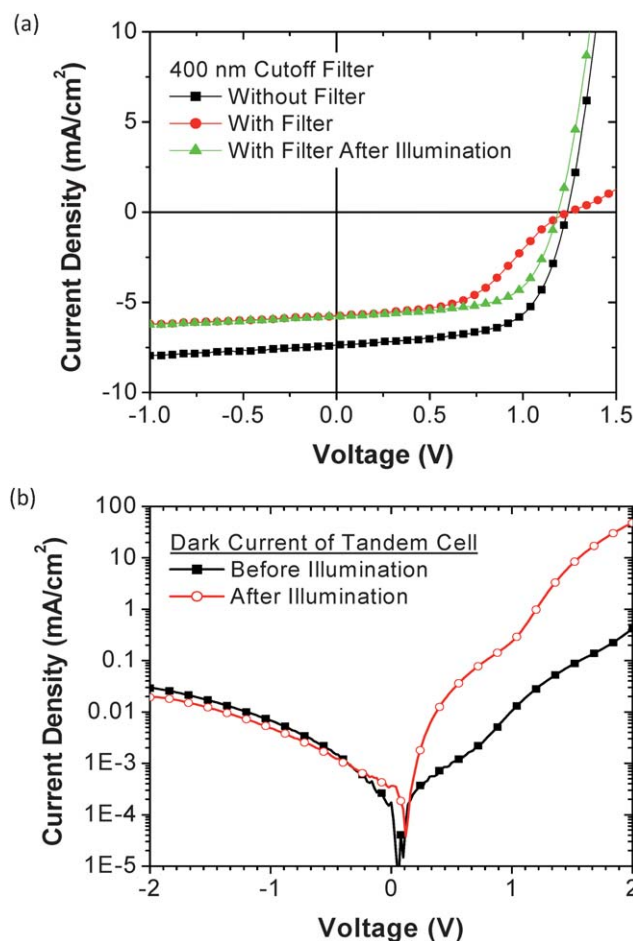


**Fig. 9** (a)  $J$ - $V$  characteristics of tandem cells under illumination with and without a 400 nm cutoff filter. With the filter s-shaped  $J$ - $V$  curves are observed that disappear when the filter is removed;<sup>30</sup> (b) dark  $J$ - $V$  characteristics of a tandem cell before and after light illumination.

have used ZnO or  $TiO_2$  *via* various processes as n-type contact and PEDOT for p-type contact, yielding efficient tandem cells.

**2.2.2 Ohmic contact between n-type and p-type layers.** Besides efficient extraction of electrons and holes from the two sub-cells, the interlayer should also act as an efficient recombination zone for the collected carriers. Any barrier to charge carriers recombination will lead to accumulation of carriers in the interlayer, increases series resistance of the device, and even may induce significant hump in the current density–voltage ( $J$ - $V$ ) curves close to  $V_{OC}$ .<sup>54</sup>

Gilot *et al.* observed an inflection point in the  $J$ - $V$  characteristics under light as shown in Fig. 8 for the tandem cell, resulting in low FF, and also loss in  $V_{OC}$ .<sup>36</sup> This was attributed to the non-Ohmic contact between ZnO and PEDOT and the interlayer forms a counterdiode resulting in reduction of voltage. In previous reports researchers used a thin metal layer which assists in efficient recombination of electrons and holes.<sup>43</sup> Following this approach when a thin Ag layer is inserted between ZnO and PEDOT layer,  $V_{OC}$  of tandem cell increased and the s-shaped curve disappears. Alternatively an Ohmic contact between n-type and p-type layers can be formed by heavily doping the two layers. PEDOT already being a heavily doped conducting polymer, the

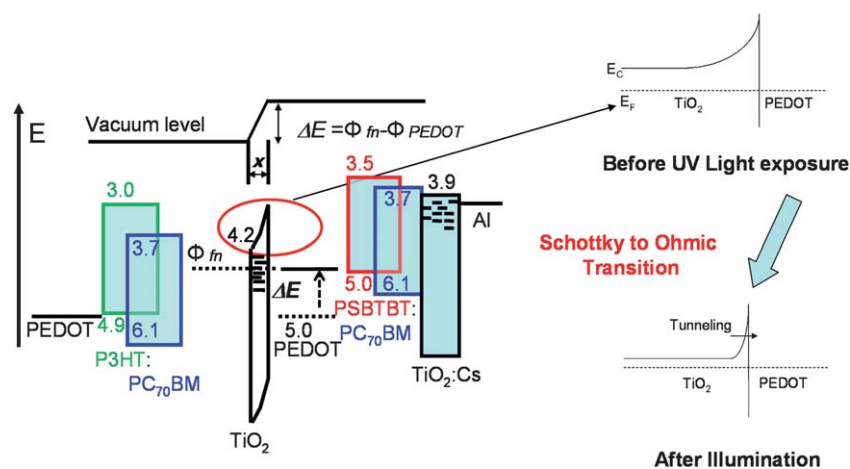


**Fig. 10** Energy band diagram of a tandem cell and the schottky to Ohmic transition at the interface between TiO<sub>2</sub> and PEDOT upon irradiating with UV light.

doping level of ZnO was increased by irradiating with UV light. Gilot *et al.* observed that the s-shaped curve disappears soon after UV irradiation and the  $V_{OC}$  of the tandem cell increases.<sup>36</sup>

Sista *et al.* also observed a pronounced s-shape in the  $J-V$  characteristics of tandem cells, as shown in Fig. 9(a), when TiO<sub>2</sub> nanoparticle layers were used for the n-type contact and PEDOT as the p-type contact.<sup>30</sup> When the cell was irradiated with UV light of wavelength below 400 nm, the s-shape disappears and FF of the device increases from 30% to over 60%. This was accompanied by an increase in the forward bias injection current by two orders of magnitude as shown in Fig. 9(b). This UV activated phenomenon is a useful hint enabling us to study the interface contact between TiO<sub>2</sub> and PEDOT. A similar behavior was observed for single cells with TiO<sub>2</sub>/PEDOT/Al as the cathode contact, confirming that this transition from a high resistance state to a low resistance state is attributable to the Schottky-to-Ohmic transition of PEDOT/TiO<sub>2</sub> contact. PEDOT being heavily p-doped and TiO<sub>2</sub> an n-type semiconductor, form a metal–semiconductor contact with a triangular barrier at the TiO<sub>2</sub>/PEDOT interface, as shown in Fig. 10. At a low doping level of TiO<sub>2</sub>, a triangular barrier width is large, creating a barrier for electrons in TiO<sub>2</sub> to recombine with holes in PEDOT. After irradiating with UV light, the free carrier concentration in TiO<sub>2</sub> significantly increases and the barrier width decreases to an extent that electrons can tunnel through the triangular barrier without any potential loss. Though this transition to Ohmic contact is not reversible over shorter time scales, the tandem cell reverts back to the high resistance state after prolonged storage in the dark.

Alternative methods to dope ZnO or TiO<sub>2</sub> should be used so that doped metal oxides are more stable. One approach is chemical doping using electron donating species. Park *et al.* were able to dope nanoparticles of TiO<sub>2</sub> by addition of Cs<sub>2</sub>CO<sub>3</sub> to the TiO<sub>2</sub> solution, causing a significant energy level shift of TiO<sub>2</sub>.<sup>50</sup> It was observed that, due to charge transfer from Cs, Ti ions were partially reduced, thus increasing the n-type doping.

To conclude this section it is important that n-type and p-type layers form an Ohmic contact for efficient carrier recombination besides forming Ohmic contacts with the polymer sub-cells. Further characterization of contact behaviors in a p–n junction

based interlayer is desirable to obtain a better understanding of the working mechanism, and a guide to the design of effective interlayers in tandem cells.

**2.2.3 Conductivity of the interlayer.** In the previous section it was mentioned that heavily doped n-type and p-type layers are necessary to form an Ohmic contact between the n-type and p-type layers, but it is not necessary to have very high conductivity interlayers. CLEVIOS P VP AI 4083, a low conductivity PEDOT, has a conductivity of 0.1 S m<sup>-1</sup> that is sufficient for use in the interlayer of a tandem solar cell. Further increase in conductivity in the PEDOT layer results in a significant charge collection outside of active area defined by electrodes overlap in the lateral direction. Since the conductive PEDOT layer is in between the two subcells, its lateral conductivity leads to an increase in the effective area of the solar cells. Sista *et al.* showed that when high conductivity PEDOT, the conductivity of which is close to 10<sup>3</sup> S m<sup>-1</sup>, is used in the interlayer, the  $J_{SC}$  from the tandem cell is overestimated by 10%. Fig. 11 compares the  $J-V$  characteristics of a single cell with the top cathode structure of

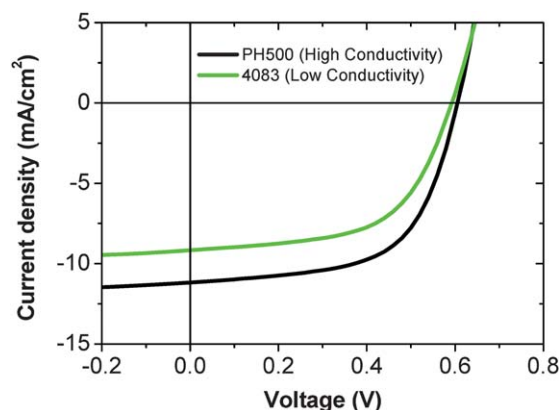


**Fig. 11**  $J-V$  characteristics of P3HT:PCBM single cells (ITO/PEDOT/P3HT:PC<sub>70</sub>BM/UT-Al\*/TiO<sub>2</sub>/PEDOT4083/Al) for high conductivity PEDOT (PH500) and low conductivity PEDOT (PEDOT 4083) as the cathode contact.<sup>30</sup> UT-Al represents 5 Ångström thick Al to enhance wettability of polymer BHJ surface.



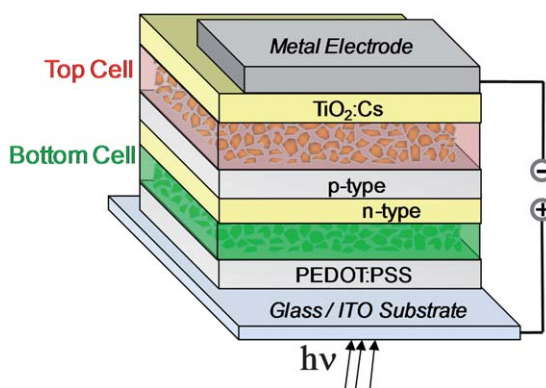


**Fig. 12** Layer by layer tandem PV device structure consisting of the bottom and top active layers and the interlayer made up of n-type and p-type layers.

TiO<sub>2</sub>/PEDOT:PSS/Al, for a low conductivity and a high conductivity PEDOT. When a high conductivity PEDOT is used instead of a low conductivity PEDOT the  $J_{SC}$  increases by 20%, while no difference in EQE for the two cells was observed.

Therefore, if high conductivity interlayers are used, the efficiency of a tandem cell can be accurately measured only if the overlap area between the interlayer and bottom ITO anode is equal to the overlap area between the interlayer and top cathode.

### 2.3 Processing issues of polymer tandem cells

One of the major challenges in fabricating polymer tandem cells is layer-by-layer solution processibility without washing away the underlying layers. Initial efforts in polymer tandem cell fabrication utilized thick and robust thermally evaporated interlayers that can sustain the solution process of the top polymer layer and protect the bottom polymer layer. These dry coated interlayers include sputter deposited ITO or thermally evaporated semi-transparent metal layers such as Au. Fully solution processed tandem cells are more challenging. A typical polymer tandem cell, shown in Fig. 12, has at least four solution processed layers that include the two polymer layers and n-type and p-type layers in the interlayer. One approach is to use orthogonal solvents so that solution processing of one layer does not affect the layer underneath. An n-type layer using ZnO or TiO<sub>2</sub> is coated from an alcohol based solvent that does not dissolve the polymer BHJ. The p-type layer is an aqueous based PEDOT that does not damage the metal oxide layer and the bottom polymer layer. Most polymers for solar cell application are soluble in chlorinated organic solvents such as dichlorobenzene, chloroform *etc.* Therefore, it is difficult to find a solvent for the top polymer layer that does not dissolve the bottom polymer layer. However, if the interlayer is thick and robust, during the solution process of the top polymer layer, the bottom polymer layer remains intact. One concern raised by Sista *et al.* is that use of high boiling point solvents for the top polymer layer may be detrimental to the integrity of underlying layers, because of the long drying time of the solvent. For this reason they used chloroform (a low boiling point solvent) for the top polymer layer, so that the solvent drying process is faster and does not penetrate the interlayer. There are reports by other researchers who have successfully

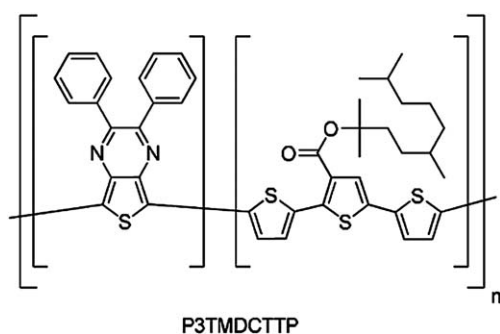


**Fig. 13** Chemical structure of the thermocleavable polymer in which the solubilizing alkyl chain is connected to the polymer backbone through an ester bond.<sup>56</sup> Reprinted with permission from reference 56. Copyright 2008 Elsevier B.V.

used high boiling point solvents for the top polymer layer when thick (10–15 nm) metal oxide layers such as MoO<sub>3</sub> are used in the interlayer.<sup>38</sup> However, minor  $V_{OC}$  loss cannot be avoided, since the metal oxide films prepared by thermal deposition or solution processes are not dense enough to resist solvent penetration. Tseng *et al.* were able to fabricate multilayer polymer light emitting diodes using an intermediate liquid buffer layer that protects the layer underneath during the spin coating process.<sup>55</sup> These approaches can be considered as alternatives to fabricate polymer tandem cells.

The approach taken by Hagemann *et al.* is to use thermocleavable materials that can be converted into insoluble films upon thermal treatment, and thus isolate the bottom subcells from further solvent processes.<sup>56</sup> Typically the solubility of the polymers can be increased using alkyl side chains that are directly attached to the polymer backbone. Hagemann *et al.* used polymer with solubilizing alkyl side groups that are linked to the polymer backbone through an ester bond. The chemical structure of the polymer is shown in Fig. 13. This ester bond breaks on thermal treatment leaving an insoluble polymer film. Though the reported efficiency is still far lower than normal polymer tandem solar cells, there is still large space for PV performance improvement of the thermocleavable polymer layers.

In layer-by-layer fabrication of tandem cells, the wettability of the surface is another issue. Polymer films are hydrophobic in nature, and sometimes, surface modification may be required to deposit the next layer. One of the purposes of TiO<sub>2</sub> film coated on top of polymer film is to convert the surface into a hydrophilic surface, so that deposition of the aqueous PEDOT is convenient.<sup>29</sup> Sista *et al.*<sup>30</sup> showed that the hydrophobic P3HT surface can be modified into hydrophilic surface by depositing a 5-Å-thick Al layer, facilitating the deposition of n-type TiO<sub>2</sub> nanoparticles. In that case, both coverage of TiO<sub>2</sub> layer on top of P3HT film surface, and energy alignment between TiO<sub>2</sub> and polymer BHJ can be significantly improved.

On the other hand, some organic solvents, *e.g.* alcoholic solvents, are compatible with both hydrophobic and hydrophilic surfaces. Aqueous PEDOT solution diluted by alcohols has better wettability on hydrophobic polymer films.<sup>44</sup> With these successful approaches based on in-depth understanding of surface and interface, more building blocks are becoming available to construct tandem cells.

## 2.4 Device characterization & modeling

In a series connected tandem cell the two sub-cells are optically and electrically coupled to each other and optimization of the tandem cell performance requires optimization of the photocurrent generation in both sub-cells. A direct approach to optimize tandem cell performance is to characterize the sub-cells independently. Yang *et al.* studied the photovoltaic behavior of the sub-cells independently in tandem architecture by wiring out a conducting metal interlayer.<sup>57</sup> However, in an actual tandem cell the embedded interlayer is non-conductive and independent characterization of sub-cells is difficult. Therefore it is necessary to adopt optical and electrical simulation approaches to explore the efficiency potential of tandem solar cells. Also, EQE measurement of the sub-cells in the tandem architecture gives information on the photocurrent-limiting sub-cell and helps in maximizing the tandem cell efficiency. However, EQE characterization for two terminal tandem photovoltaic cells needs to be modified<sup>29</sup> compared to the conventional method for single junction solar cells.<sup>58</sup>

**2.4.1 Optical/electrical modeling.** Due to lack of any experimental techniques to characterize the sub-cells independently, optical and electrical simulation techniques are strong tools to optimize tandem cells. These tools simplify the complexity of experimental approach to optimize tandem cells by varying the thickness of the active layers. Thin film optics for multilayered structures such as polymer solar cells is well established<sup>59</sup> and can be extended to tandem cells in calculating optical field distribution for varying thickness of the two sub-cells.<sup>60,61</sup> As a first step refractive index ( $n$ ) and extinction coefficient ( $k$ ) of all the layers in a tandem cell are obtained using multiple wavelength/angle mode ellipsometry measurements. Using these measured values, a quantitative estimation of the number of absorbed photons in each active layer can be obtained as a function of thickness of each sub-cell. Optical simulation gives information on exciton generation profile in organic layers. Electrical simulations can be done on tandem structures to get information on photocurrent generation provided information on the e-h pair dissociation efficiency and recombination rates is known for the BHJs.<sup>62</sup>

Gilot *et al.* used the optical simulation results and internal quantum efficiency (IQE) data of single junction cells to calculate the photocurrent generated in each sub-cell.<sup>61</sup> Further, they demonstrated a generalized approach to estimate the  $J$ - $V$  characteristics of the tandem cell from the  $I$ - $V$  curves of dummy sub-cells. When a tandem cell is operated under 1 sun condition, the light intensity received by the sub-cells is less than 1 sun and depends on the optical field distribution. The  $J$ - $V$  curve of dummy sub-cell was obtained by measuring the  $J$ - $V$  curve of the corresponding single cell operated under same light intensity condition as it would be for the sub-cell in a tandem configuration. The coupling of  $J$ - $V$  curves of two sub-cells generates  $J$ - $V$  curves in good agreement with measured  $J$ - $V$  curves of the tandem cells.

In the electrical simulation done by Gilot *et al.* it was assumed that the interlayer acts as an efficient recombination zone.<sup>35,61</sup> However, with non-ideal interlayers, additional resistance and charge recombination barriers should be considered, resulting in complication in electrical simulation.<sup>54</sup> Therefore, to maximize

tandem cell efficiencies, the choice of an efficient interlayer is as important as materials for sub-cells and device optimization. From an efficiency point of view, this issue should be minimized, and requires ideal interlayers.<sup>63</sup>

**2.4.2 Accurate PCE and EQE characterization.** Accurate characterization of PCE is essential in fair comparison of efficiencies reported by different research groups. In case of single junction solar cells, spectral mismatch of the solar simulator has to be corrected in order to estimate the PCE accurately.<sup>58</sup> In case of tandem cells, another source of efficiency overestimation arises from the conductivity of the interlayer. It has been realized that high conductivity interfacial layers between electrodes and polymer films induce charge collection along lateral direction, raising the concern of efficiency overestimation.<sup>64</sup> We have shown that high conductivity interfacial layers may not be a prerequisite to an efficient interlayer in tandem structure.<sup>30</sup> Even normal PEDOT 4083 with a conductivity of  $10^{-1}$  s  $m^{-1}$  can be used to construct highly efficient tandem cells. It should be noted that using a high conductivity interconnection layer may result in efficiency overestimation for both front and rear sub-cells. On the other hand in case of three<sup>65,66</sup> or four terminal cells,<sup>67</sup> since the efficiency measurement of individual sub-cells is not correlated, the situation is same as single BHJ cell characterization.<sup>57</sup>

EQE measurement is a commonly used technique to estimate the  $J_{SC}$  of single cells accurately. This approach can be extended to tandem cells as well for accurate estimation of  $J_{SC}$  delivered by the tandem cell. Another advantage of measuring the EQE of the sub-cells is that the current limiting cell can be identified and improvements can be made to optimize the tandem cell performance. However, measuring EQE of tandem cells using the standard EQE characterization method for single cells is not viable, since the sub-cells work in a collaborative way to utilize different part of solar spectrum and the optical response of each sub-cell in tandem structure should be balanced over the entire solar spectrum and not necessarily at a specific wavelength. The inorganic solar cell community has adopted a modified EQE measurement technique that requires additional voltage biasing and light biasing.<sup>68</sup> This modified EQE technique was extended to polymer tandem cells by Kim *et al.* with some simplification.<sup>29</sup> They used monochromatic light bias that selectively excites one sub-cell such that it is saturated while probing EQE of the other sub-cell. The bias light wavelength is chosen such that the sub-cell under test has negligibly small absorption at that wavelength.

However, it should be noted that EQE measurement using this method is appropriate for the case in which the two sub-cells have shunt resistance large enough such that photocurrent at a finite negative bias does not vary significantly from the short circuit point. Fig. 14 shows the  $J$ - $V$  characteristics of the tandem cell, the current limiting sub-cell and optically biased sub-cell. Since the optically biased sub-cell is saturated, a finite photovoltage ( $V_+$ ) develops across it. Under the short circuit condition of the tandem cell, a equal amount of negative bias ( $V_-$ ) is induced across the current limiting sub-cell. Therefore the EQE of the current limiting sub-cell is in reality being measured under reverse bias conditions. This leads to overestimation of EQE value if the photocurrent is sensitive to the applied bias, as shown in Fig. 14.

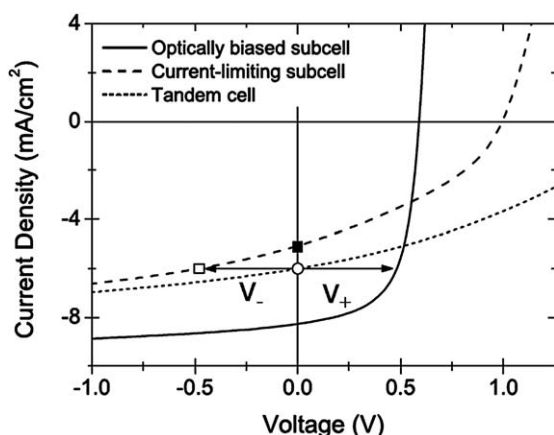


**Fig. 14**  $J$ - $V$  characteristics of the tandem cell, optically biased sub-cell and current limiting sub-cell. The photocurrent of the current limiting cell that is measured from EQE measurements (denoted by the open square) is higher than actual  $J_{SC}$  (denoted by filled square).<sup>69</sup> Reprinted with permission from reference 69. Copyright 2010 Wiley VCH.

Gilot *et al.* corrected for this inconsistency and reported an accurate method of determining the EQE of the sub-cells under 1 sun condition and at short-circuit conditions.<sup>69</sup> They considered two important aspects of the current limiting sub-cell while determining the EQE (a) non-linear light intensity dependence of photocurrent and (b) reverse bias voltage dependence. A combination of light bias and voltage bias was applied for accurate estimation of EQE. Intensity of the light bias was chosen to simulate 1 sun condition for the current limiting sub-cell. A positive bias was applied across the tandem cell to compensate for the negative voltage induced across the current limiting sub-cell. The magnitude of the positive bias was determined from dummy  $J$ - $V$  characteristics that were predicted from optical simulations of the tandem cell, making EQE characterization closer to the real working condition of the sub-cell.

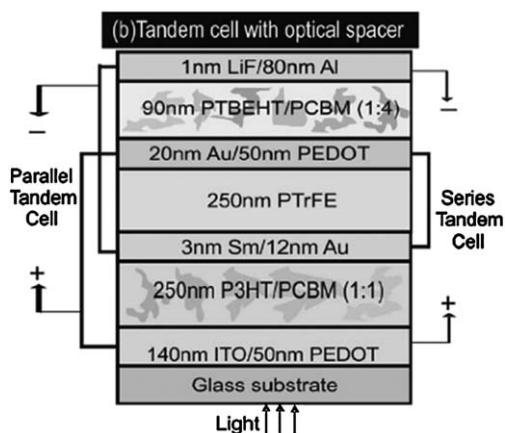


**Fig. 15** Four terminal tandem cell demonstrated by Hadipour *et al.* The cathode contact to the bottom cell and the anode contact to the top cell are conductive and semitransparent contacts made using thin Au layer, and an insulating optical spacer is used to isolate the two Au layers. The two cells can be connected in series or in parallel.<sup>67</sup> Reprinted with permission from reference 67. Copyright 2007 American Institute of Physics.

### 3 Novel tandem structures

Besides the two terminal tandem cells, other novel tandem or stacked structures have been demonstrated each having their own advantages.

#### 3.1 Multi terminal tandem cells

In a two terminal tandem cell, the two sub-cells are connected in series through an interlayer. The current delivered by the tandem cell is governed by Kirchoff's law and is limited by the cell that delivers the lowest current. In the case where one of the polymer cells delivers a higher current, the thickness of the polymer layer should be reduced to match the current with the second cell delivering a lower photocurrent. Unless the two component cells that constitute a tandem cell deliver equal photocurrent under their optimized single cell configurations, incorporating them in a tandem cell will possibly lead to some efficiency losses. A more ideal tandem cell configuration would be when the two component cells can be operated separately, so that the efficiency of the tandem cell is simply the addition of efficiencies of the two subcells.

Hadipour *et al.* demonstrated a four terminal tandem cell as shown in Fig. 15, where the two polymer sub-cells were separated by an optical spacer.<sup>67</sup> The bottom cell was semitransparent with transparent ITO anode and semi-transparent Au cathode, while the top cell had a semitransparent Au anode and a reflecting cathode. The two semi-transparent Au electrodes were separated by an insulating optical spacer. In this configuration the two sub-cells can be connected either in series or in parallel depending upon the polarity of the four terminals, as shown in Fig. 15.

In this device structure the amount of photocurrent generated by the top cell is much less than that by the bottom cell and the  $V_{OC}$  of the component cells are similar. When connected in series, the  $J_{SC}$  of tandem cell is very low, resulting in a low efficiency tandem cell. On the other hand, the parallel connected cell has much better performance than the series connected cell, because of no loss in the  $V_{OC}$  and the added-up current. Also there is no requirement on photocurrent matching for parallel connection tandem cell.

Sista *et al.* demonstrated a 3-terminal tandem structure,<sup>65</sup> shown in Fig. 16, in which two subcells are connected in parallel through a transparent conducting interlayer that acts as a common electrode to the two subcells. The unique advantage of

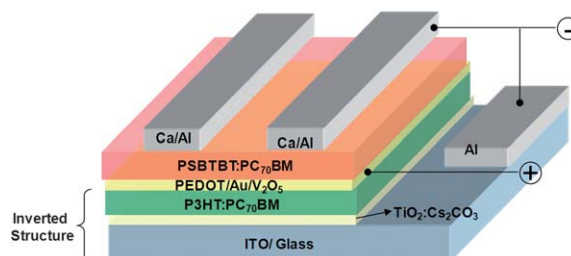


**Fig. 16** Schematic of the three terminal polymer tandem cell with transparent conducting interlayer acting as a common anode for the two sub-cells. The interlayer can be wired out to measure the efficiency of the bottom and top cell independently and as well as when connected in parallel.

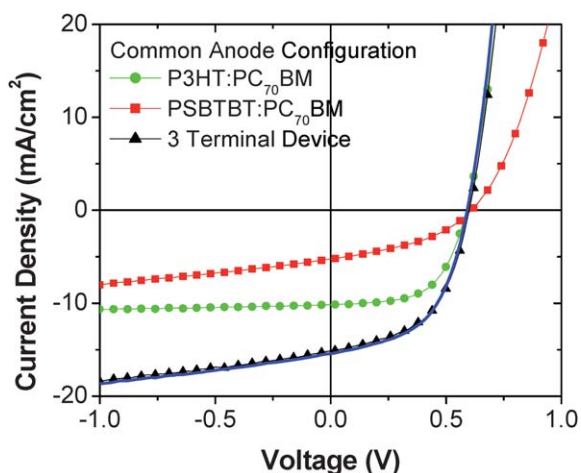


**Fig. 17** Current density–voltage ( $J$ – $V$ ) characteristics of front P3HT:PC<sub>70</sub>BM cell (circle), rear PSBTBT:PC<sub>70</sub>BM cell (square) and parallel connected tandem cell (triangles) under Am 1.5 G (100 mW cm<sup>-2</sup>) of light illumination for common anode configuration. The estimated  $J$ – $V$  characteristics (solid line) of the tandem cell calculated by adding the current densities of the single cells at different voltage bias matches exactly with the measured  $J$ – $V$  characteristics of the tandem cell.<sup>65</sup> Reprinted with permission from reference 65. Copyright 2010 Wiley VCH.

this device structure is that the two sub-cells can be characterized independently and as well as when connected in parallel and no photocurrent matching criterion is required. Unlike a 2-terminal tandem cell, the interlayer used in 3-terminal tandem device collects only one kind of carriers (either electron or holes) from both bottom and top cell. Secondly the interlayer should have high conductivity so that the carriers can be extracted efficiently to the external circuit. P3HT:PC<sub>70</sub>BM was used as the large band gap cell and PSBTBT:PC<sub>70</sub>BM as the low band gap cell. A 10 nm thick Au layer was used as semi-transparent and conductive interlayer. The interlayer can be used as common anode to collect holes or common cathode to collect electrons depending on the surface modification of the Au layer. For common anode configuration, Au surface was modified with high work function vanadium pentoxide (V<sub>2</sub>O<sub>5</sub>) and for common cathode configuration the Au surface was modified with low work function TiO<sub>2</sub> doped Cs<sub>2</sub>CO<sub>3</sub>. Fig. 17 shows the  $J$ – $V$  characteristics of the sub-cell and parallel connected tandem cell for the common anode configuration. The parallel connected tandem cell delivered  $J_{SC}$  of 15.1 mA cm<sup>-2</sup> which was equal to the sum of  $J_{SC}$  of the component cells. The FF of parallel connected tandem cell was dominated by the cell that delivers the largest current which in this case is the front P3HT:PC<sub>70</sub>BM cell. The rear cell delivers very low  $J_{SC}$  because of the optical losses encountered in the semi-transparent interlayer. Because of the conductive nature of the interlayer, it should be ensured that the active area of the top and bottom cells is equal when connected in parallel.

Tandem cells in parallel connection have been reported by Tanaka *et al.*<sup>70</sup> and Guo *et al.*<sup>66</sup> as well. Tanaka *et al.* used multiwalled carbon nanotube (MWCNT) sheet modified with PEDOT as the anode interlayer. They used P3HT:PCBM as then bottom cell and top small molecule cell based on CuPc and C<sub>60</sub>. They observed an increase in the  $J_{SC}$  for the tandem cell, though

**Table 1** Summary of the photovoltaic parameters for the parallel connected cell demonstrated by Guo *et al.*<sup>66</sup>

	$J_{SC}/\text{mA cm}^{-2}$	$V_{OC}/\text{V}$	PCE (%)	FF (%)
Front sub-cell	6.49	0.65	1.45	34
Rear sub-cell	4.25	0.60	1.24	49
Tandem Cell	11.32	0.65	3.1	42

this was not equal to the sum of  $J_{SC}$  of the component cells. This loss in  $J_{SC}$  for tandem cell was attributed to the interface resistance between MWCNT sheet and the organic layers.

Xie's group demonstrated parallel connected polymer tandem cells using P3HT:PCBM and PCPDTBT:PCBM as the component cells.<sup>66</sup> The transparent conductive layer based on Al(2 nm)/Ag(15 nm) was modified with 10 nm thick MoO<sub>3</sub> layer on either side to form a anode contact for the top and bottom cells. The PV parameters of the two sub-cells and the parallel connected tandem cell are summarized in Table 1. The efficiency of the tandem cell is slightly higher than the sum of the efficiencies of the two sub-cells. This is attributed to the decrease in series resistance when the two sub cells are connected in parallel, showing the advantage of a highly conductive metal as a middle electrode.

### 3.2 Inverted tandem cells

PEDOT:PSS and n-type metal oxides are commonly used as the interfacial functional layer between the photoactive polymer and metal contacts. PEDOT has been used to improve the anode contact with ITO;<sup>71</sup> however, its acidic nature etches the ITO and imposes potential lifetime instability.<sup>72–74</sup> Furthermore, previous studies revealed PEDOT to be an inefficient electron-blocking layer due to electron leakage at the anode. Beside the potential instability, optical loss due to absorption of the PEDOT film approaches 10% in the visible range, and even higher in the near infrared (NIR) region.<sup>75</sup>

Consequently, metal oxides with higher stability and optical transparency have been proposed to replace PEDOT as the interfacial layer between ITO and polymer BHJs.<sup>76</sup> These functional interlayers can be used to modify the ITO work function to collect either electrons or holes. For example, inverted cells were fabricated where the workfunction of ITO was reduced using an

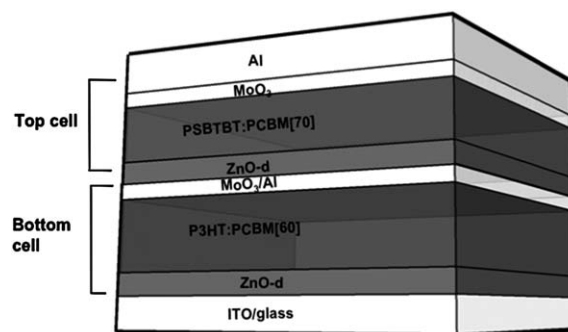


**Fig. 18** The device structure of the inverted tandem cell, with the metal-oxide interlayer (MoO<sub>3</sub>/Al/ZnO-d) connecting the two subcells.<sup>81</sup>

ultrathin  $\text{Cs}_2\text{CO}_3$  layer such that it becomes the cathode to extract electrons.<sup>77,78</sup> Furthermore the vertical phase separation observed in certain polymer-PCBM blends, where the bottom electrode is acceptor-rich and the top surface donor-rich, is favorable for inverted structure. In an inverted architecture the anode is composed of a relatively stable hole collection layer covered by a high work function metal. The absence of PEDOT and low work function metals implies promising long term stability of the inverted structure. Other prominent examples of the inverted structure utilized electron transport layers with good hole blocking properties, such as  $\text{TiO}_2$ ,<sup>53,79</sup>  $\text{TiO}_2 : \text{Cs}_2\text{CO}_3$ ,<sup>50</sup> or  $\text{ZnO}$ <sup>51,52,80</sup> atop ITO.

Recently Chou *et al.* combined the advantages of both the tandem and inverted structure by employing a metal oxide-only interlayer ( $\text{MoO}_3/\text{Al}/\text{ZnO}$ ) to connect two polymer BHJs (P3HT:PC<sub>60</sub>BM and PSBTBT:PC<sub>70</sub>BM subcells) as shown in Fig. 18, achieving an inverted tandem solar cell with PCE of 5.1%.<sup>81</sup> A low temperature hydrolysis process was developed to form a dense and smooth amorphous ZnO layer with excellent diode properties, while the crystalline ZnO appears rougher and more porous. In addition, the  $\text{MoO}_3$  provides a much robust resilience against the sol-gel process compared to  $\text{V}_2\text{O}_5$  or Al, which results in poor charge selectivity and thus the s-shaped  $J-V$  behavior.<sup>54</sup> As a result, the materials and configurations of the interlayer for the tandem architecture were no longer limited by the acidic PEDOT. Compared to PEDOT, the absorption of the metal oxide-based interlayer is also negligible throughout the visible to NIR spectral range (transmittance > 95%), resulting in a high photocurrent for both single and tandem cells.

Coincidentally, Sun *et al.* reported a multi-layered connection in inverted tandem cells.<sup>82</sup>  $\text{MoO}_3/\text{Ag}/\text{Al}/\text{Ca}$  interlayer was vacuum deposited, and followed by deposition of the rear cell *via* spin-coating process. Such an interlayer structure features high transparency and low series resistance, as well as effective charge recombination, rendering an exact summation of  $V_{oc}$  (1.18 V) of the two subcells and a high fill factor (61.8%). Maximum PCE of 2.78% is mainly due to the fact of using identical subcells.

### 3.3 Other novel tandem structures (folded tandem cell & lateral tandem cell)

One of the main challenges in fabricating a monolithic polymer tandem cell is the layer-by-layer deposition using solution process. To overcome the hassle of solution processibility of monolithic tandem cells, some researchers have employed novel approaches of stacking two polymer BHJ fabricated on two different substrates.

Shrotriya *et al.* fabricated a stacked structure of polymer cells such that the two cells can be connected in series or in parallel.<sup>83</sup> In this stacked structure, the bottom cell was semi-transparent so that the unabsorbed light in the bottom cell can be transmitted through the transparent cathode and absorbed by the top cell. A multilayer of lithium fluoride (LiF)/aluminium (Al)/gold (Au) was used as the semi-transparent contact to the bottom cell. Since the two cells are connected electrically in series or in parallel using an external wire, the efficiency values were doubled over efficiency of single cells. However, the transmittance of the semi-transparent cathode for wavelengths more than 600 nm is

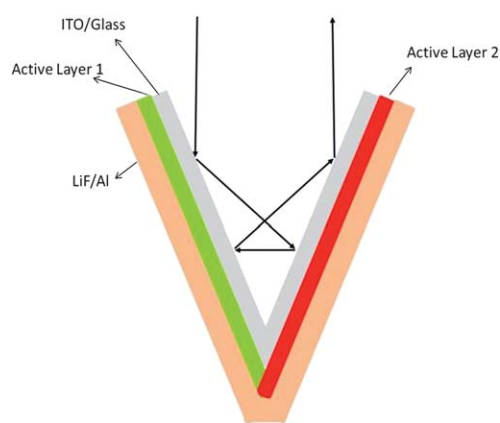


**Fig. 19** Schematic of the folded tandem cell where in two cells fabricated on different substrates are placed at an angle. Light that is unabsorbed and reflected by large band gap cell is absorbed by the second low band gap cell.<sup>85</sup>

less than 80%, making this structure less efficient for low band gap cells.

In 2007 there were two simultaneous reports by Rim *et al.*<sup>84</sup> and Tvingstedt *et al.*<sup>85</sup> on v-shaped or folded tandem cell. In this structure two polymer BHJ with reflective cathodes are placed at an angle to each other, as shown in Fig. 19. The unabsorbed light by one cell after reflection is directed towards the second cell where it is absorbed. In this folded configuration the light is trapped due to multiple reflections from the two reflecting surfaces as a result of which the absorption is enhanced. Rim *et al.* modeled the absorption enhancement for different cell in the v-shaped configuration. They showed that for small molecule cell based on CuPc the absorption increases by over three times. The absorption enhancement is lower for single cells that have high absorption efficiency such as that for P3HT:PCBM cells. Also the absorption increase is dependent on the angle between the two cells. Tvingstedt *et al.* used two alternating copolymers of fluorine (AFPO) with different band gaps on each face of the v-shaped structure.<sup>85</sup> These cells were tested when connected in series or parallel and the performance was evaluated for different angles between the two cells. They showed that the PCE increases from 2.0% to 3.7% when the angle between the two cells is changed 180° to 40°. Zhou *et al.* extended this concept of folded geometry to multiple folded cells on plastic substrates.<sup>86</sup> They were able to achieve a  $V_{oc}$  of 3.65V when four cells in a W-shaped geometry were connected in series.

Another new concept proposed by Kim *et al.*<sup>87</sup> is that of lateral tandem cell. In this configuration a dispersive-focusing element (DFE) is used to split the incoming solar photons spectrally such that light of different wavelength is incident at a different position in the lateral direction as shown in Fig. 20. The sub-cells of the lateral tandem cell are placed laterally and have a continuously varying absorption profile. The position of each sub-cell is varied in such a way that each sub-cell resonantly excites the wavelength of photons incident at that position. Theoretically PCE exceeding 18% can be achieved when ideal DFE and microcavity sub-cells are used. Though the concept of a lateral tandem cell is very interesting, realizing such a tandem cell is both extremely challenging and may not be cost-effective due to the use of DFEs.

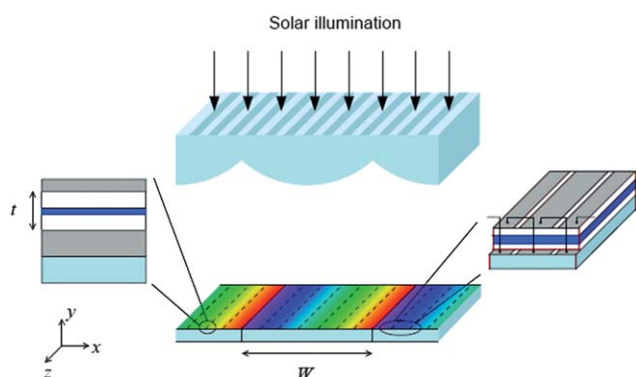


**Fig. 20** Lateral tandem cell utilizing a DMF to split the incident white light spectrally and an array of sub-cells with continuously varying resonant cavity wavelength stacked laterally. The wavelength of light incident at a specific position is such that it resonates with the cavity of the sub-cell at that position.<sup>87</sup> Reprinted with permission from reference 87. Copyright 2008 Optical Society of America.

In addition to the above-mentioned structures, simple tandem cells utilizing the advantages of 2-terminal cells, have been reported recently.<sup>63</sup> Chen *et al.* has proposed that spray-coating offers layer-by-layer deposition through a solution process without dissolving the underlying layer. It is convenient to construct an interlayer free tandem photovoltaic cell, stacking two polymer BHJs sequentially using a novel multi-source spray coating process. Therefore, the photoresponse range covers absorption bands of the two BHJs from 300 nm to 840 nm. PCE approaching 3% has been obtained. More importantly, efficient energy transfer from the large bandgap polymer to the low bandgap one was observed, suggesting the possibility of realization of the photo-recycling concept<sup>88</sup> in polymer tandem solar cells.

Similarly, polymer solar cells based on multilayer structures prepared by thermal lamination have been reported by Nakamura *et al.*<sup>89</sup> The broadened light absorption range of the multilayer devices compared to that of single-layer P3HT:PCBM devices improved the  $J_{SC}$ . Hence PCE improvement was observed. Furthermore, it is claimed that the recombination rate at the interfaces was largely affected by the stacking order of the layers, resulting in the difference of the FFs, indicating interfaces between polymer BHJs play an important role in such a structure.

#### 4. Conclusion

With the recent breakthroughs in organic/polymeric photovoltaic research,<sup>17,18</sup> it is believed that 10% conversion efficiency can be reached for single cells in the near future. The next target for the whole field would be at least 15%. Achieving such high efficiencies based on single junction is extremely challenging because of the trade-off between photocurrent gain and loss in  $V_{OC}$  when band gap is lowered. Considering the intrinsic limitation of single junction cell, reduction in electrical potential loss should therefore be the critical issue in the photon-to-electron conversion process in photovoltaic cells.

Therefore to achieve efficiencies close to 15%, the application of tandem architectures for organic/polymeric solar cells offers

us many advantages. Recent efforts in polymer tandem cells have shown enhanced tandem cell efficiencies compared to the constituent sub-cells. Layer-by-layer deposition can be realized *via* surface and interface engineering, and a vast range of efficient interfacial and photoactive materials are available. Various new approaches and device design have been proposed to enhance tandem cell performance, offering opportunity to incorporate newly synthesized low bandgap materials to achieve breakthrough efficiencies. Currently organic tandem cells have relatively complicated structures compared to single junction cells, raising concerns about processibility issues. For example, vacuum deposition is still a major method for fabrication, though all solution processed structures are highly desirable. The compromise between simple process/structures and high efficiency<sup>63</sup> has to be reached with respect to future applications.

#### 5. Acknowledgement

The financial support for the tandem solar cell research is from the following organizations: Air Force Office of Scientific Research (Dr Charles Lee, Program Manager), Office of Naval Research (Dr Paul Armistead, Program Manager), Solarmer Energy Inc., University of California Discovery Grant for financial support. The authors would also like to thank Dr Hua-Hsien Liao (Enli Technology) for his technical support and discussion.

#### References

- 1 D. M. Chapin, C. S. Fuller and G. L. Pearson, *J. Appl. Phys.*, 1954, **25**, 676.
- 2 Y. S. Tsuo, T. H. Wang and T. F. Ciszek, presented in part at the Electrochemical Society Annual Meeting, Seattle, Washington, May 3 1999.
- 3 W. W. Hou, B. Bob, S.-H. Li and Y. Yang, *Thin Solid Films*, 2009, **517**, 6853.
- 4 A. Goetzberger, C. Hebling and H. W. Schock, *Mat Sci Eng R*, 2003, **40**, 1.
- 5 D. Mitzi, M. Yuan, W. Liu, A. Kellock, S. Chey, L. Gignac and A. G. Schrott, *Thin Solid Films*, 2009, **517**, 2158.
- 6 S.-S. Sun and N. S. Sariciftci, ed., *Organic Photovoltaics: Mechanisms, Materials and Devices*, CRC Press, Boca Raton, FL, 2005.
- 7 C. J. Brabec, V. Dyakonov, J. Parisi, N. S. Sariciftci, ed., *Organic Photovoltaics: Concepts and Realization*, Springer, Berlin, Germany, 2003.
- 8 G. Dennler, M. C. Scharber and C. J. Brabec, *Adv. Mater.*, 2009, **21**, 1323.
- 9 G. Li, V. Shrotriya, J. S. Huang, Y. Yao, T. Moriarty, K. Emery and Y. Yang, *Nat. Mater.*, 2005, **4**, 864.
- 10 F. Padinger, R. S. Rittberger and N. S. Sariciftci, *Adv. Funct. Mater.*, 2003, **13**, 85.
- 11 G. Li, V. Shrotriya, Y. Yao, J. S. Huang and Y. Yang, *J. Mater. Chem.*, 2007, **17**, 3126.
- 12 J. Peet, J. Y. Kim, N. E. Coates, W. L. Ma, D. Moses, A. J. Heeger and G. C. Bazan, *Nat. Mater.*, 2007, **6**, 497.
- 13 Y. Y. Liang, D. Q. Feng, Y. Wu, S. T. Tsai, G. Li, C. Ray and L. P. Yu, *J. Am. Chem. Soc.*, 2009, **131**, 7792.
- 14 J. H. Hou, H. Y. Chen, S. Q. Zhang, G. Li and Y. Yang, *J. Am. Chem. Soc.*, 2008, **130**, 16144.
- 15 H.-Y. Chen, J. Hou, S. Zhang, Y. Liang, G. Yang, Y. Yang, L. Yu, Y. Wu and G. Li, *Nat. Photonics*, 2009, **3**, 649.
- 16 M.-H. Chen, J. Hou, Z. Hong, G. Yang, S. Sista, L.-M. Chen and Y. Yang, *Adv. Mater.*, 2009, **21**, 4238.
- 17 'Solarmer Energy Inc. breaks psychological barrier with 8.13% OPV efficiency', <http://www.solarmer.com/news.php>.
- 18 'Heliatek and IAPP achieve production-relevant efficiency record for organic photovoltaic cells', <http://www.heliatek.com/index.php?page=news>.

- 19 M. C. Scharber, D. Wuhlbacher, M. Koppe, P. Denk, C. Waldauf, A. J. Heeger and C. L. Brabec, *Adv. Mater.*, 2006, **18**, 789.
- 20 'NREL solar cell sets world efficiency record at 40.8 percent', <http://www.nrel.gov/news/press/2008/625.html>.
- 21 M. Hiramoto, M. Suezaki and M. Yokoyama, *Chem. Lett.*, 1990, 327.
- 22 G. Dennler, H. J. Prall, R. Koeppel, M. Egginger, R. Autengruber and N. S. Sariciftci, *Appl. Phys. Lett.*, 2006, **89**, 073502.
- 23 A. Colmann, J. Junge, C. Kayser and U. Lemmer, *Appl. Phys. Lett.*, 2006, **89**, 203506.
- 24 A. G. F. Janssen, T. Riedl, S. Hamwi, H. H. Johannes and W. Kowalsky, *Appl. Phys. Lett.*, 2007, **91**, 073519.
- 25 D. W. Zhao, X. W. Sun, C. Y. Jiang, A. K. K. Kyaw, G. Q. Lo and D. L. Kwong, *Appl. Phys. Lett.*, 2008, **93**, 083305.
- 26 B. J. Lee, H. J. Kim, W.-I. Jeong and J.-J. Kim, *Sol. Energy Mater. Sol. Cells*, 2010, **94**, 542.
- 27 K. Kawano, N. Ito, T. Nishimori and J. Sakai, *Appl. Phys. Lett.*, 2006, **88**, 073514.
- 28 A. Hadipour, B. de Boer, J. Wildeman, F. B. Kooistra, J. C. Hummelen, M. G. R. Turbiez, M. M. Wienk, R. A. J. Janssen and P. W. M. Blom, *Adv. Funct. Mater.*, 2006, **16**, 1897.
- 29 J. Y. Kim, K. Lee, N. E. Coates, D. Moses, T. Q. Nguyen, M. Dante and A. J. Heeger, *Science*, 2007, **317**, 222.
- 30 S. Sista, M.-H. Park, Z. Hong, Y. Wu, J. Hou, W. L. Kwan, G. Li and Y. Yang, *Adv. Mater.*, 2010, **22**, 380.
- 31 A. Hadipour, B. de Boer and P. W. M. Blom, *Adv. Funct. Mater.*, 2008, **18**, 169.
- 32 T. Ameri, G. Dinnler, C. Lungenschmied and C. J. Brabec, *Energy Environ. Sci.*, 2009, **2**, 347.
- 33 G. Dennler, M. C. Scharber, T. Ameri, P. Denk, K. Forberich, C. Waldauf and C. J. Brabec, *Adv. Mater.*, 2008, **20**, 579.
- 34 J. Yang, R. Zhu, Z. Hong, Y. He, A. Kumar, Y. Li and Y. Yang, manuscript submitted and under revision.
- 35 A. Hadipour, B. d. Boer and P. W. M. Blom, *Org. Electron.*, 2008, **9**, 617.
- 36 J. Gilot, M. M. Wienk and R. A. J. Janssen, *Appl. Phys. Lett.*, 2007, **90**, 143512.
- 37 D. W. Zhao, X. W. Sun, C. Y. Jiang, A. K. K. Kyaw, G. Q. Lo and D. L. Kwong, *IEEE Electron Device Lett.*, 2009, **30**, 490.
- 38 J. Sakai, K. Kawano, T. Yamanari, T. Taima, Y. Yoshida and A. Fujii, *Sol. Energy Mater. Sol. Cells*, 2010, **94**, 376.
- 39 G. Dennler, K. Forberich, T. Ameri, C. Waldauf, P. Denk and C. J. Brabec, *J. Appl. Phys.*, 2007, **102**, 123109.
- 40 H.-Y. Chen, J. Hou, A. E. Hayden, H. Yang, K. N. Houk and Y. Yang, *Adv. Mater.*, 2009, 371.
- 41 X. Guo, F. Liu, B. Meng, Z. Xie and L. Wang, *Org. Electron.*, 2010, **11**, 1230.
- 42 Y.-C. Chen, C.-Y. Yu, C.-P. Chen, S.-H. Chan and C. Ting, *J. Sol. Energy Eng.*, 2010, **132**, 021103.
- 43 A. Yakimov and S. R. Forrest, *Appl. Phys. Lett.*, 2002, **80**, 1667.
- 44 H.-J. Prall, R. Koeppel, R. Autengruber, M. Egginger, G. Dennler and N. S. Sariciftci, *Proc. SPIE*, vol. 6197, San Diego, 2006.
- 45 J. Drechsel, B. Mannig, F. Kozlowski, M. Pfeiffer, K. Leo and H. Hoppe, *Appl. Phys. Lett.*, 2005, **86**, 244102.
- 46 R. Timmreck, S. Olthof, K. Leo and M. K. Riede, *J. Appl. Phys.*, 2010, **108**, 033108.
- 47 D. W. Zhao, X. W. Sun, C. Y. Jiang, A. K. K. Kyaw, G. Q. Lo and D. L. Kwong, *Appl. Phys. Lett.*, 2008, **93**, 083305.
- 48 V. Shrotriya, G. Li, Y. Yang, C.-W. Chu and Y. Yang, *Appl. Phys. Lett.*, 2006, **88**, 073508.
- 49 A. Hayakawa, O. Yoshikawa, T. Fujieda, K. Uehara and S. Yoshikawa, *Appl. Phys. Lett.*, 2007, **90**, 163517.
- 50 M. H. Park, J. H. Li, A. Kumar, G. Li and Y. Yang, *Adv. Funct. Mater.*, 2009, **19**, 1241.
- 51 N. Sekine, C.-H. Chou, W. L. Kwan and Y. Yang, *Org. Electron.*, 2009, **10**, 1473.
- 52 S. K. Hau, H. L. Yip, N. S. Baek, J. Y. Zou, K. O'Malley and A. K. Y. Jen, *Appl. Phys. Lett.*, 2008, **92**, 253301.
- 53 M. S. White, D. C. Olson, S. E. Shaheen, N. Kopidakis and D. S. Ginley, *Appl. Phys. Lett.*, 2006, **89**, 143517.
- 54 A. Kumar, S. Sista and Y. Yang, *J. Appl. Phys.*, 2009, **105**, 094512.
- 55 S.-R. Tseng, S.-C. Lin, H.-F. Meng, H.-H. Liao, C.-H. Yeh, H.-C. Lai, S.-F. Horng and C.-S. Hsu, *Appl. Phys. Lett.*, 2006, **88**, 163501.
- 56 O. Hagemann, M. Bjerring, N. C. Nielsen and F. C. Krebs, *Sol. Energy Mater. Sol. Cells*, 2008, **92**, 1327.
- 57 H. B. Yang, Q. L. Song, C. M. Li and Z. S. Lu, *Energy Environ. Sci.*, 2008, **1**, 389.
- 58 V. Shrotriya, G. Li, Y. Yao, T. Moriarty, K. Emry and Y. Yang, *Adv. Funct. Mater.*, 2006, **16**, 2016.
- 59 P. Peumans, A. Yakimov and S. R. Forrest, *J. Appl. Phys.*, 2003, **93**, 3693.
- 60 N.-K. Persson and O. Inganas, *Sol. Energy Mater. Sol. Cells*, 2006, **90**, 3491.
- 61 J. Gilot, M. M. Wienk and R. A. J. Janssen, *Adv. Mater.*, 2010, **22**, E67.
- 62 G. Namkoong, P. Bolans, K. Lee and J. Dean, *J. Appl. Phys.*, 2010, **107**, 124515.
- 63 L.-M. Chen, Z. Hong, W. L. Kwan, C.-H. Lu, Y.-F. Lai, B. Lei, C.-P. Liu and Y. Yang, *ACS Nano*, 2010.
- 64 M.-S. Kim, M.-G. Kang, L. J. Guo and J. Kim, *Appl. Phys. Lett.*, 2008, **92**, 133301.
- 65 S. Sista, Z. Hong, M.-H. Park, Z. Xu and Y. Yang, *Adv. Mater.*, 2010, **22**, E77.
- 66 Z. Guo, F. Liu, W. Yue, Z. Xie, Y. Geng and L. Wang, *Org. Electron.*, 2009, **10**, 1174.
- 67 A. Hadipour, B. d. Boer and P. W. M. Blom, *J. Appl. Phys.*, 2007, **102**, 074506.
- 68 M. Meusel, C. Baur, G. Letay, A. W. Bett, W. Warta and E. Fernandez, *Progr. Photovolt.: Res. Appl.*, 2003, **11**, 499.
- 69 J. Gilot, M. M. Wienk and R. A. J. Janssen, *Adv. Funct. Mater.*, 2010, **20**, 3904.
- 70 S. Tanaka, K. Mielczarek, R. Ovalle-Robles, B. Wang, D. Hsu and A. A. Zakhidov, *Appl. Phys. Lett.*, 2009, **94**, 113506.
- 71 Y. Cao, G. Yu, X. Zhang, R. Menon and A. J. Heeger, *Synth. Met.*, 1997, **87**, 171.
- 72 M. P. d. Jong, L. J. v. Izendoorn and M. J. A. d. Voigt, *Appl. Phys. Lett.*, 2000, **77**, 2255.
- 73 Y. H. Kim, S.-H. Lee, J. Noh and S.-H. Han, *Thin Solid Films*, 2006, **510**, 305.
- 74 K. W. Wong, H. L. Yip, Y. Luo, K. Y. Wong, W. M. Lau, K. H. Low, H. F. Chow, Z. Q. Gao, W. L. Yeung and C. C. Chang, *Appl. Phys. Lett.*, 2002, **80**, 2788.
- 75 S. C. Meskers, J. K. J. v. Duan and R. A. J. Janssen, *Adv. Funct. Mater.*, 2003, **13**, 805.
- 76 V. Shrotriya, G. Li, Y. Yao, C. W. Chu and Y. Yang, *Appl. Phys. Lett.*, 2006, **88**, 073508.
- 77 G. Li, C.-W. Chu, V. Shrotriya, J. Huang and Y. Yang, *Appl. Phys. Lett.*, 2006, **88**, 253503.
- 78 H.-H. Liao, L.-M. Chen, Z. Xu, G. Li and Y. Yang, *Appl. Phys. Lett.*, 2008, **92**, 173303.
- 79 G. K. Mor, K. Shankar, M. Paulose, O. K. Varghese and C. A. Grimes, *Appl. Phys. Lett.*, 2007, **91**, 152111.
- 80 C. Waldauf, M. Morana, P. Denk, P. Coakley, S. A. Choulis and C. J. Brabec, *Appl. Phys. Lett.*, 2006, **89**, 233517.
- 81 C.-H. Chou, W. L. Kwan, Z. Hong, L.-M. Chen and Y. Yang, *Adv. Mater.*, 2010.
- 82 X. W. Sun, D. W. Zhao, L. Ke, A. K. K. Kyaw, G. Q. Lo and D. L. Kwong, *Appl. Phys. Lett.*, 2010, **97**, 053303.
- 83 V. Shrotriya, E. H.-E. Wu, G. Li, Y. Yao and Y. Yang, *Appl. Phys. Lett.*, 2006, **88**, 064104.
- 84 S.-B. Rim, S. Zhao, S. R. Scully, M. D. McGehee and P. Peumans, *Appl. Phys. Lett.*, 2007, **91**, 243501.
- 85 K. Tvingstedt, V. Andersson, F. Zhang and O. Inganas, *Appl. Phys. Lett.*, 2007, **91**, 123514.
- 86 Y. Zhou, F. Zhang, K. Tvingstedt, W. Tian and O. Inganas, *Appl. Phys. Lett.*, 2008, **93**, 033302.
- 87 C. Kim and J. Kim, *Opt. Express*, 2008, **16**, 19987.
- 88 J. Nelson, *The Physics of Solar Cells*, Imperial College Press, London, 2003.
- 89 M. Nakamura, C. Yang, E. Zhou, K. Tajima and K. Hashimoto, *ACS Appl. Mater. Interfaces*, 2009, **1**, 2703.